Master 2 Training Period Report

Numerical investigation of the size effects on the exchange bias in nanostructures

CEA Grenoble, DRFMC
SPINTEC

Mihai GABOR

Coordinator : Bernard DIENY

Contents

1 Introduction

This training period toked place at *CEA Grenoble*, at the *Direction des Sciences de la Matičre (DSM)*, *Département de Recherche Fondamentale sur la Matičre Condensée (DRFMC)*, at the *Laboratoire de Spintronique et Technologie des Composants (SPINTEC)* in colaboration with *Laboratoire de Simulation Atomistique (L_Sim)*. The coordinator of this internship was Mr. Bernard Dieny to whom I want to thank for his support and valuable discussions. I am also grateful to Mr. Frédéric Lançon (L_Sim) for receiving me into his group and for useful discussions. I would also like to thank to Thomas Jourdan for all his assistance during this internship and to the entire team of the *L_Sim* laboratory.

1.1 Scientific context of the study

Research into antiferromagnetic AFM materials has seen a great increase since the invention and implementation of spin valve giant magnetoresistance sensors [1]. Exchange bias materials in thin film form have been the most widely studied type of system. The exchange anisotropy between the antiferromagnet (AFM) and ferromagnet (FM) leads to a unidirectional anisotropy which shifts the hysteresis loop of the FM layer from zero axis by an amount referred to as the exchange field, H_E.

The industrial demand to systematically reduce the size of spin valve and other exchange bias based devices has triggered the interest in the research of exchange biased nanostructures. From the more basic point of view, it is well known that a range of remarkable properties arise, in both FM and AFM materials, as the size is reduced, hence it is appealing to investigate how does size reduction affect FM/AFM coupled systems.

It is clearly, now, that the exchange bias phenomena it is strictly correlated to the AFM domain structure [13],[6][2]. The reduction of the lateral dimensions of an exchange biased system down to length scales comparable to FM or AFM magnetic domain sizes is also interesting from a fundamental point of view since this results in a confinement and subsequent alteration of the FM and AFM domain structures, hence allowing us to probe the role of domains on exchange bias.

1.2 Training period objectives

The main objective of this internship was to study the finite size effects on the exchange bias in an AFM/FM bilayer using atomistic numerical simulations.

The simulation were done using a program (*Mi_Magnet*) developed at *L_Sim* by Frédéric Lançon and Luc Billard. The scripts were written using *Python* ® program-

ming language. The replicated systems had a lateral size between 7 and 100nm, and the AFM layer thickness was varied between 2 and 10nm.

2 Theoretical aspects

2.1 Exchange bias in FM/AFM thin films

Discovered in 1956 by Meiklejohn and Bean [12], exchange bias refers to the unidirectional pinning of a ferromagnetic layer by an adjacent antiferromagnet. Ferromagnetic films typically have a preferred magnetization axis, *easy axis*, and the spins prefer to align along this axis. There are two equally stable easy spin directions (rotated by 180^o) along this axis and it costs the same energy and requires the same external field to align the spins along either easy direction. As shown on the left side of fig. 2.1 the magnetization loop is therefore symmetric about zero. When a ferromagnet (FM) is

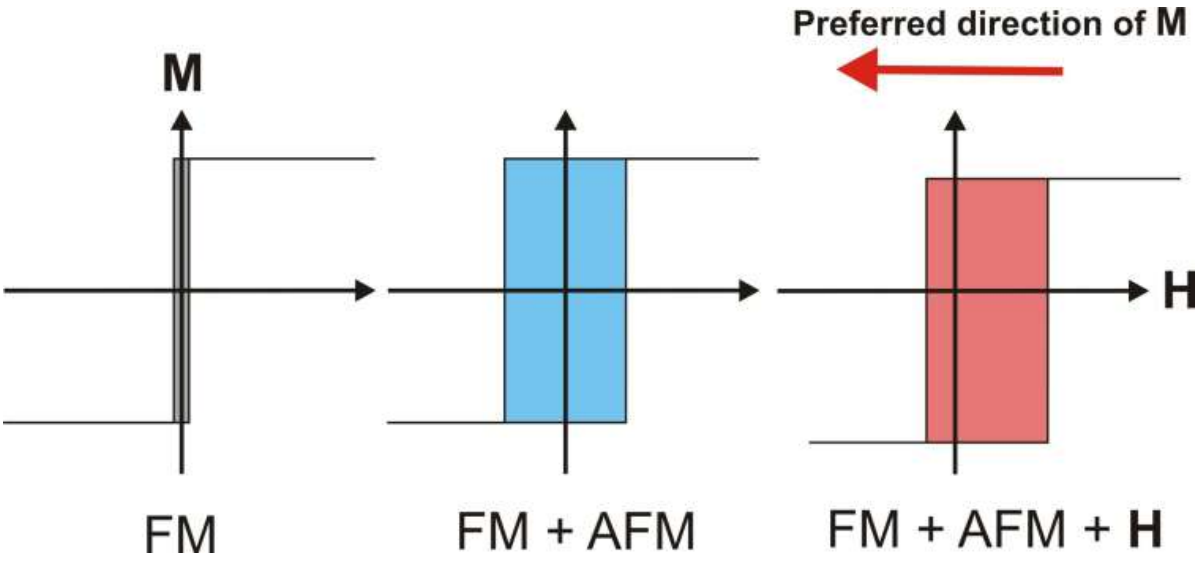

Fig. 2.1: *Easy axis magnetization loops of ferromagnetic (FM) film (left), a FM film grown on an antiferromagnet (AFM) (middle), and a FM/AFM sandwich grown in a field H or annealed in a field H above the Neel temperature (right). In the right structure the FM is said to be biased.*

grown on an antiferromagnet (AFM) the exchange coupling between the two systems leads to an increased coercivity of the ferromagnet (fig. 2.1 middle). The ferromagnetic hysteresis loop is still symmetric, indicating two equivalent easy directions. If, on the other hand, the AFM/FM system is grown in a magnetic field or after growth annealed in a magnetic field to temperatures above the AFM Neel temperature, the hysteresis loop becomes asymmetric and is shifted from zero (fig. 2.1 right). This unidirectional

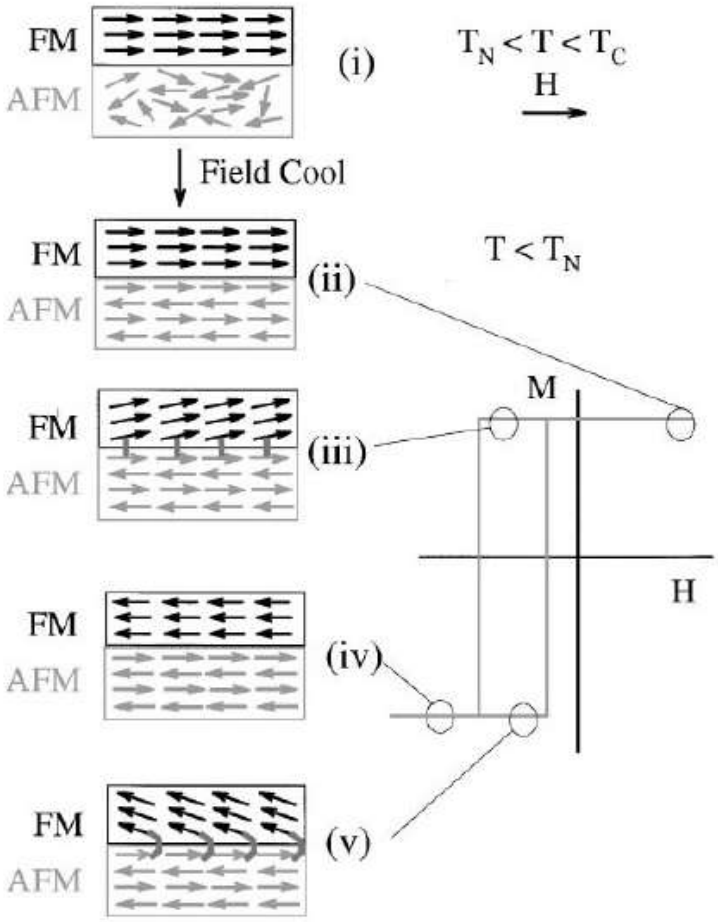

Fig. 2.2: *Schematic representation of the different stages taking place in a FM/AFM system hysteresis cycle*

shift is called exchange bias and reflects the fact that there is now a preferred easy magnetization direction for the FM.

It must be noted that if the FM/AF system is not *field cooled* no shift in the hysteresis loop will appear.

Qualitatively the exchange bias phenomena can be understood as follows (fig. 2.2): ff $T_N < T < T_C$ (where T_N is the Néel temperature of the AFM and T_C is the Curie temperature of the FM) the ferromagnetic layer will be magnetically ordered, and if a field is applied the FM spins line up with the field, and in the same time the AFM layer will be paramagnetic, so if the field is weak enough, the AFM spins is remain random (fig. 2.2 (i)). If the sample temperature is decreased bellow the Néel temperature of the AFM (fig. 2.2 (ii)), the spins of the AFM will start to order antiferromagnetically, with respect to, the magnetically ordered, ferromagnetic spins. At a temperature lower than T_N, in negative applied field, the spins of the FM layer will start to rotate, while, for sufficiently large AFM anisotropy, the spins of the AFM layer will remain fixed (fig. 2.2

(iii)). Therefore, the interfacial interaction between the FM/AFM spins tries to align ferromagnetically the FM spins with the AFM spins at the interface. In other words, the AFM spins at the interface exert a microscopic torque on the FM spins, to keep them in their original position (ferromagnetically aligned at the interface). Therefore, the FM spins have one single stable configuration, in other words the anisotropy is unidirectional. So, the field needed to reverse completely an FM layer will be larger if it is in contact with an AFM, because an extra field is needed to overcome the microscopic torque. However, once the field changes sign, the FM spins will start to rotate at a smaller field, due to the interaction with the AFM spins (which now exert a torque in the same direction as the field) (fig. 2.2(v)). The sample behaves as if there was an extra (internal) biasing field, therefore, the FM hysteresis loop is shifted in the field axis.

Although this simple phenomenological model gives an intuitive picture there is little quantitative understanding of this phenomena. There are several models that explain several features of the phenomena [13], but complete understanding is still lacking.

2.1.1 Meiklejohn model

Meiklejohn has developed the first model that tried to explain the exchange biasing phenomena. Using the same intuitive picture expressed in the previous section. In this model, the energy per unit area of an exchange bias system, assuming coherent rotation of the FM layer magnetization, can be written [12] as:

$$E = -HM_{FM}t_{FM}\cos(\theta-\beta) + K_{FM}t_{FM}\sin^2(\beta) + K_{AFM}t_{AFM}\sin^2(\alpha) - J_{INT}\cos(\beta-\alpha) \tag{2.1}$$

where H is the applied field, M_{FM} the saturation magnetization, t_{FM} the thickness of the FM layer, t_{AFM} the thickness of the AFM layer, K_{FM} the anisotropy of the FM layer, K_{AFM} the anisotropy of the AFM layer and J_{INT} the interface coupling constant.β, α and θ are the angles between the magnetization and the FM anisotropy axis, the AFM sublattice magnetization (M_{AFM}) and the AFM anisotropy axis, and the applied field and the FM anisotropy axis (see fig.2.3) [12]. Note that the AFM and FM anisotropy axes are usually assumed to be in the same direction (collinear). The first term in the energy equation accounts for the effect of the applied field on the FM layer, the second term is the effect of the FM anisotropy, the third term takes into account the AFM anisotropy and the last term takes into consideration the interface coupling. Although this energy function takes into account the main parameters involved in exchange bias, it assumes: the absence of AFM and/or FM domains, that the AFM and FM anisotropy axes are parallel and ferromagnetic coupling at the interface.

In the simplest case the FM anisotropy is assumed to be negligible (the condition $K_{FM}t_{FM} \ll K_{AFM}t_{AFM}$ is often fulfilled experimentally), thus the energy becomes:

$$E = -HM_{FM}t_{FM}\cos(\theta-\beta) + K_{AFM}t_{AFM}\sin^2(\alpha) - J_{INT}\cos(\beta-\alpha) \tag{2.2}$$

Minimizing the energy with respect to α and β the loop shift is found to be:

$$H_E = \frac{J_{INT}}{M_{FM}t_{FM}} \tag{2.3}$$

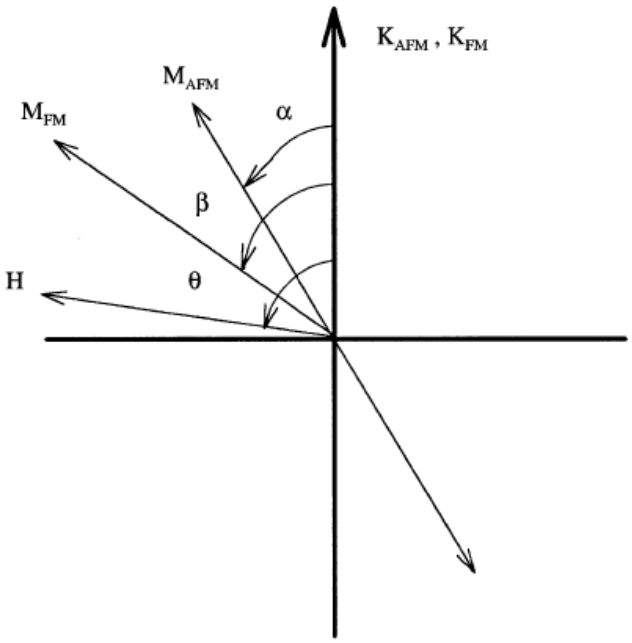

Fig. 2.3: *Schematic diagram of angles involved in an exchange bias system.Note that the AFM and FM anisotropy axes are assumed collinear and that the M_{AFM} is the magnetization of one of the AFM sublattices.*

This value represents the field needed for the Zeeman energy to overcome the interface exchange coupling energy. In order to determine the equilibrium positions of the FM and AFM spins one has to minimize the energy with respect to angles α and β:

$$\frac{\partial E}{\partial \alpha} = 0 \Rightarrow \sin 2\alpha = \frac{J_{INT}}{K_{AFM} t_{AFM}} \sin(\beta - \alpha) \tag{2.4}$$

$$\frac{\partial E}{\partial \beta} = 0 \Rightarrow \sin(\beta - \alpha) = \frac{H M_{FM} t_{FM}}{J_{INT}} \sin(\beta - \alpha) \tag{2.5}$$

An important result from this minimization is that the condition:

$$K_{AFM} t_{AFM} \geq J_{INT} \tag{2.6}$$

is required for the observation of exchange anisotropy. If $K_{AFM} t_{AFM} \gg J_{INT}$ then is more energetically favorable to keep α small independently of β. However, if $K_{AFM} t_{AFM} \ll J_{INT}$ it is energetically favorable able to keep $(\beta - \alpha)$ small, i.e. AFM and FM spins rotate together. In other words, if the above condition is not satisfied, the AFM spins follow the motion of the FM layer, thus no loop shift should be observed, only an increase in coercivity. The exchange bias magnitude predicted by these calculations depends on the assumed value for J_{INT}. If J_{INT} is chosen to be similar to the ferromagnetic exchange constant then H_E is predicted to be several orders of magnitude larger than the experimental results ([14]).

2.1.2 Mauri model

To explain the discrepancy between the exchange field value predicted by simple theory and experimental observations, Mauri et al.([3]) proposed a mechanism that would effectively lower the interfacial energy cost of reversing the FM layer without removing the condition of strong interfacial FM/AFM coupling. The model propose the formation of a planar domain wall in the AFM once the the FM reverses its orientation (see fig. 2.4). The AFM domain wall length calculation is the same as for a ferromagnetic Bloch

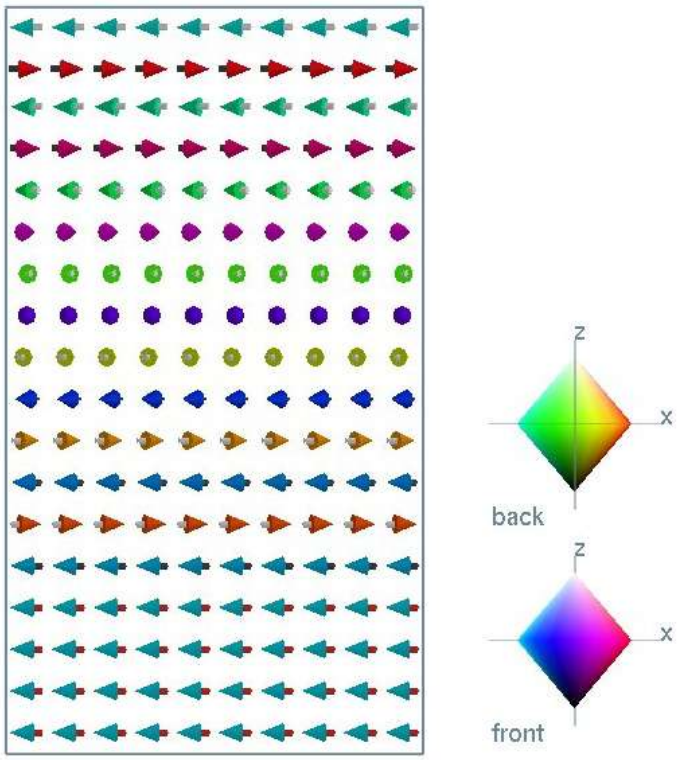

Fig. 2.4: *Schematic representation of the domain wall, formed in the AFM by the by the FM magnetization rotation process*

domain wall([4]):

$$\delta = \pi\sqrt{\frac{A_{AFM}}{K_{AFM}}} \tag{2.7}$$

and the energy:

$$\Delta E = \pi\sqrt{A_{AFM}K_{AFM}} \tag{2.8}$$

So in this model the interaction energy, between the two materials, is no longer confined at the interface but spread across the width of the domain wall, and thus reducing H_E by an amount proportional with $\pi\sqrt{A_{AFM}K_{AFM}}/a$ (≈ 100). This new value will prove to be consisted with the experimental observed ones.

It is convenient to distinguish between two limiting cases:

- strong interfacial coupling, for which:

$$H_E = 2\left(\frac{\sqrt{A_{AFM}K_{AFM}}}{M_{FM}t_{FM}}\right) \tag{2.9}$$

- weak interfacial coupling, for which:

$$H_E = -\left(\frac{J_{INT}}{M_{FM}t_{FM}}\right) \tag{2.10}$$

where J_{INT} is the effective interfacial coupling energy, and t_{FM} and M_{FM} are the thickness and saturation magnetization of the FM, respectively. In the case of strong interfacial exchange coupling, H_E saturates at energies far less than the fully uncompensated interfacial exchange coupling due to the formation of an AFM domain wall. In the case of weak interfacial exchange coupling H_E is limited by the strength of the interfacial exchange coupling J_{INT} . This model highlights the formation of an AFM planar domain wall in the limit of strong interfacial exchange.

2.1.3 Malozemoff model

Although the Mauri model predicts a reasonable value for the exchange bias field, it fails to explain the persistence of H_E down to AFM thicknesses of that are an order of magnitude smaller than the characteristic domain wall width[12],[8]. In order to count for this Malozemoff argued that an ideal interface was unrealistic and structural roughness would lead to magnetic defects giving rise to a local random field([9],[10],[11]). If one considers a simple atomic step at the interface then a part of the AFM spins will be frustrated (due to the ferromagnetic coupling with the FM spins) and this will lead to the formation of an AFM perpendicular domain wall (fig. 2.5). For interfacial roughness that is random on the atomic scale, the local unidirectional interface energy σ_l is also random:

$$\sigma_l = \pm\frac{zJ_{INT}}{a^2} \tag{2.11}$$

where, a the lattice parameter, z is the coordination number. Random-field theory stipulates that a net average non-zero interfacial energy will exist when the average is taken over a small number of sites. Statistically, the average σ in an area of L^2 will decrease as $\sigma_l/\sqrt{N}$ where $N = L^2/a^2$ is the number in that area.

Using the random field formalism, Malozemoff showed that it is energetically favorable for the AFM to break up into domainlike regions and he obtained for the exchange anisotropy field:

$$H_E = \frac{2z\sqrt{A_{AFM}K_{AFM}}}{\pi^2 M_{FM}t_{FM}} \tag{2.12}$$

This equation is remarkably similar with eq. 2.9, and therefore is able to explain the order of magnitude of the exchange anisotropy effect. This similarity reflects the fact that fundamentally both models take into account domain walls formation and energies.

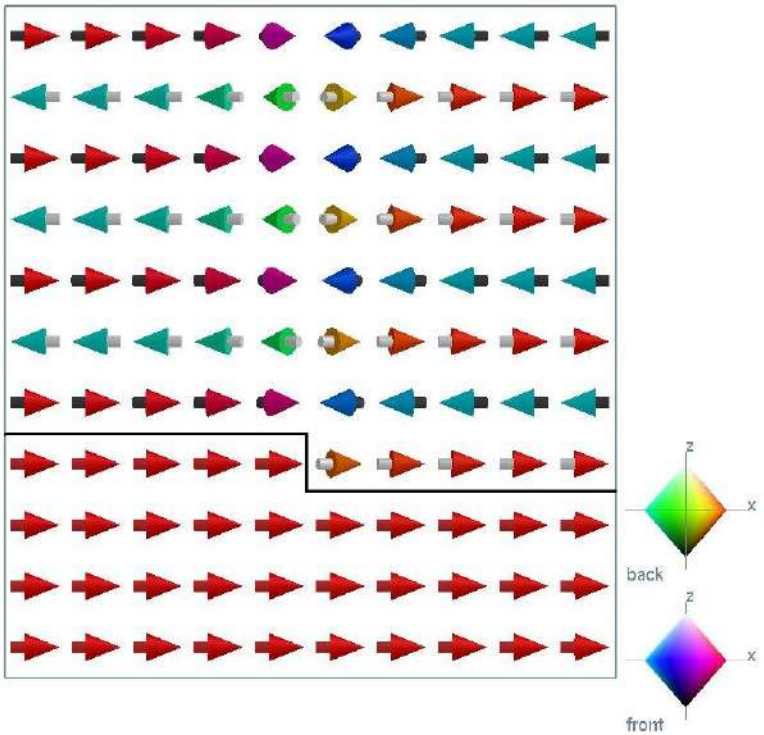

Fig. 2.5: *Schematic representation of a perpendicular domain wall, formed in the AFM by an atomic step interface roughness.*

It is important to note that there are also other models that take into account different important parameters in the exchange bias. These include random anisotropy in the AFM layer, non-collinearity of the AFM/FM spins, grain size distribution or uncompensated surface spins [13]. These models have attained different degrees of agreement with the experimental results. Often the individual approximations apply for a specific model system and are not valid for others systems.

2.2 Numerical Simulations

We have seen that there are several interpretations of the exchange bias mechanism. In order to obtain a better understanding of the phenomena, we made use of numerical simulations of the AFM/FM spins comportment. The program used for these simulations (called *Mi-Magnet*) employs an atomistic approach and was developed by Frédéric Lançon and Luc Billard from the *L_Sim* laboratory. The AFM/FM system is replicated by a simple cubic lattice with a Heisenberg spin in each node. The total energy of the

system can be thus written:

$$E = -\sum_{i,j} J_{FM}\vec{S}^i_{FM}\vec{S}^j_{FM} - \sum_{i,j} J_{AFM}\vec{S}^i_{AFM}\vec{S}^j_{AFM} - \sum_{surf} J_{INT}\vec{S}_{FM}\vec{S}_{AFM} - \sum_i \vec{H}\vec{S}^i_{FM} - \\ -\sum_i \vec{H}\vec{S}^i_{AFM} - \sum_i K_{FM}(\vec{n}_{FM}\vec{S}^i_{FM})^2 - \sum_i K_{AFM}(\vec{n}_{AFM}\vec{S}^i_{AFM})^2 \tag{2.13}$$

were we have introduced:

- the exchange interaction terms in the FM, AFM and those related to the interface
- the Zeeman energy terms associated with the external field
- the anisotropy terms for each layer

Thus the system is completely defined by the following parameters:

- the exchange interaction constants in the FM, in the AFM and at the AFM/FM interface : J_{FM}, J_{AFM}, J_{INT}
- the anisotropy directions and constants: $\vec{n}_{FM}, \vec{n}_{AFM}, K_{FM}, K_{AFM}$
- the magnetic moment of each atom: $\vec{S}_{FM}, \vec{S}_{AFM}$
- the applied magnetic field: $\vec{H}$

The *Mi_Magnet* program minimization energy algorithm works in to stages. First an axis around which the spins will be turned is determined. This axis corresponds with the direction of the torque that is exerted on each spin, in other words with the direction of $\vec{S}_i \wedge \vec{b}_i$ where $\vec{b}_i$ is the local field that exerts on each spin (it contains the Zeeman, anisotropy and exchange contributions). In the second stage the rotation angles are determined by the *conjugate gradient method*. This to steps are iterated until a sufficiently small variation in energy, that gives a good convergence, is reached .

It is important to note that we have not introduced a magnetostatic energy term. This is due to two reasons: because the size of the system, that we studied, is smaller than $100\,nm$ this term is neglectful compared to the exchange energy terms; and because the absence of this term reduces substantial the calculations time.

3 Finite size effects on the exchange bias

I order to study the finite size effects on the exchange biased bilayers we have performed numerical simulations using an atomistic model. The AFM/FM system is replicated by a simple cubic lattice with a Heisenberg spin in each node (fig. 3.1). In our calculations

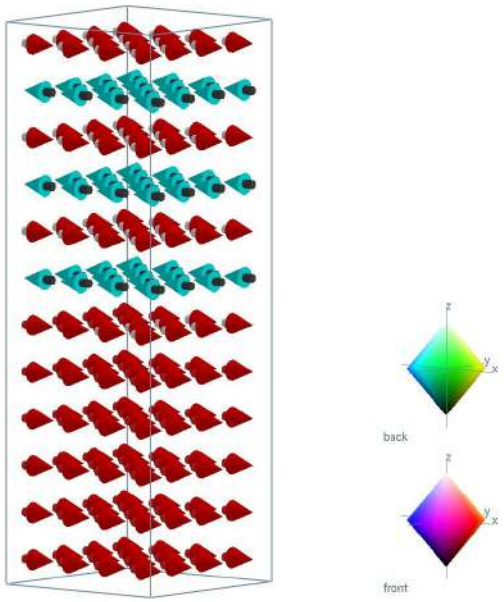

Fig. 3.1: *Replicated FM/AFM bilayer; the lattice is simple cubic lattice, with Heisenberg spins in each node; each spins stands for* $4 \times 4 \times 1$ atomic spins.

each spin stands for $4 \times 4 \times 1$ *atomic* spins.

The material parameters chosen for the AFM are those corresponding to $IrMn$ [8], so we have selected an exchange stiffness constant: $A_{AFM} = 10^{-12} J/m$ and uniaxial anisotropy constant $K_{AFM} = 1.8 \times 10^5 J/m^3$. For the FM we have piked the exchange stiffness constant to be $A_{FM} = 10 \times A_{AFM}$ and an uniaxial anisotropy constant $K_{FM} = K_{AFM}/25$, parameters describing well the permalloy (NiFe). For the interfacial exchange constant we have chosen, according with [5] a value of $J_{INT} = 0.47 J_{AFM}$.

The lattice constant value of $3,5\mathring{A}$ was kept the same for both AFM and FM.

The FM and the AFM easy anisotropy axis are taken to be parallel with themselves and with the Ox axis.

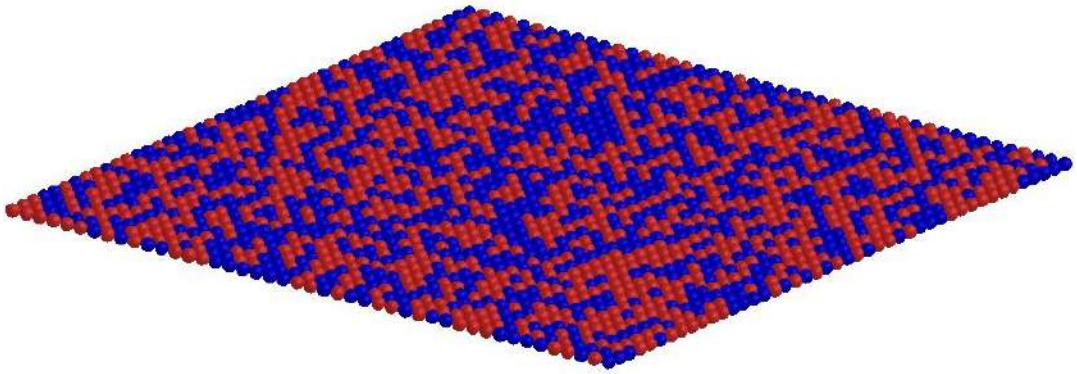

Fig. 3.2: *Simulated rough AFM/FM interface; the blue dots represent AFM* atoms*, the red ones represent FM* atoms*; each spot stands for* $4 \times 4 \times 1$ *atoms.*

The size effects study on exchange bias was made keeping the FM layer thickness constant (6 nm equivalent with 11 atomic planes) while the thickness of the AFM layer was varied between 2 an 10 nm (6 to 29 atomic planes), also the lateral dimension of the structure was swept between 7 and 100 nm (corresponding to 5 respectively 75 *atomic* planes.

Due to the the fact that each spin corresponds to $4 \times 4 \times 1$ *atomic* spins a *renormalization* of the material parameters has been done. Details on the derivation of the new parameters can be found in the appendix A. As a result we have obtained different in-plane and out-of-plane exchange constants. The in-plane exchange constant was found to be: $J_{\parallel} = J_{at}$ while the out-of-plane exchange constant: $J_{\perp} = 16 \times J_{at}$. As for the anisotropy constant we have found : $K = 16 \times K_{at}$.

In an attempt to reproduce as accurate as possible a realistic AFM/FM interface, roughness was introduced (see fig. 3.2). Hence the single atomic layer interface is randomly populated with AFM or FM *atoms*.

3.1 The AFM layer spin configuration for different lateral sizes of the system

To see the influence of reduced lateral size (LS) of the AFM/FM bilayer on the exchange bias we have calculated hysteresis cycles for different structures keeping the thickness of the AFM layer constant an varying its area.

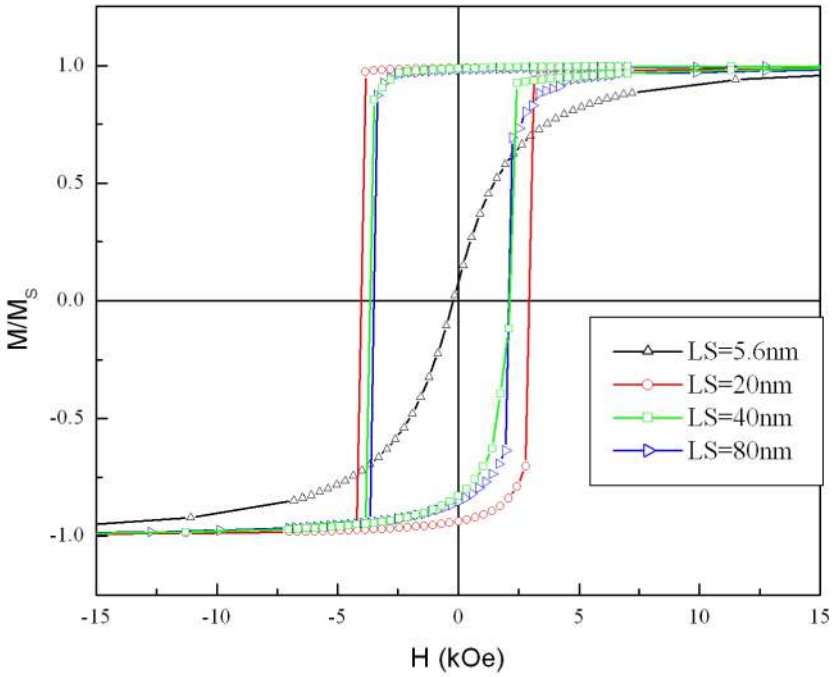

Fig. 3.3: *Hysteresis cycles for an AFM/FM bilayer with FM thickness is 6 nm, AFM thickness is 4nm and LS=15, 20, 40 and 80 nm.*

3.1.1 The system with the AFM layer thickness of 4 nm

One of the first systems simulated was that with a with a FM layer thickness of $6nm$, a AFM layer thickness of $4\,nm$ and a lateral size comprised between 5.6 and $100\,nm$. The calculated hysteresis cycles are presented in the figure 3.3 (in order to maintain the clarity of the graph only four hysteresis curve are presented). Depending on the magnitude of the system surface two types of curves are obtained. For a lateral size (LS) smaller than $20\,nm$ the curve presents no hysteresis while for LS larger than $20nm$ the hysteresis is important. This comportment is due to different spin configurations, of the AFM layer during the reversal of the magnetization of the FM layer, for different lateral sizes of the system.

It is important to note that for all the structures that we have simulated the FM will remain single-domain. In fact using the material parameters for the FM layer one can calculate the domain wall length in the FM to be $\delta_{FM} = \pi\sqrt{A_{FM}/K_{FM}} \approx 120\,nm$, thus for a $LS < 100\,nm$ the FM will remain single-domain because the physical dimensions of the FM are not enough to accommodate a domain wall.

In the figure 3.4 the spin configuration for the structure with $LS = 5.6nm$ in three different states: in positive saturation, zero applied field and negative saturation, is presented. One can see, from the figure, that the FM remains a single domain (the

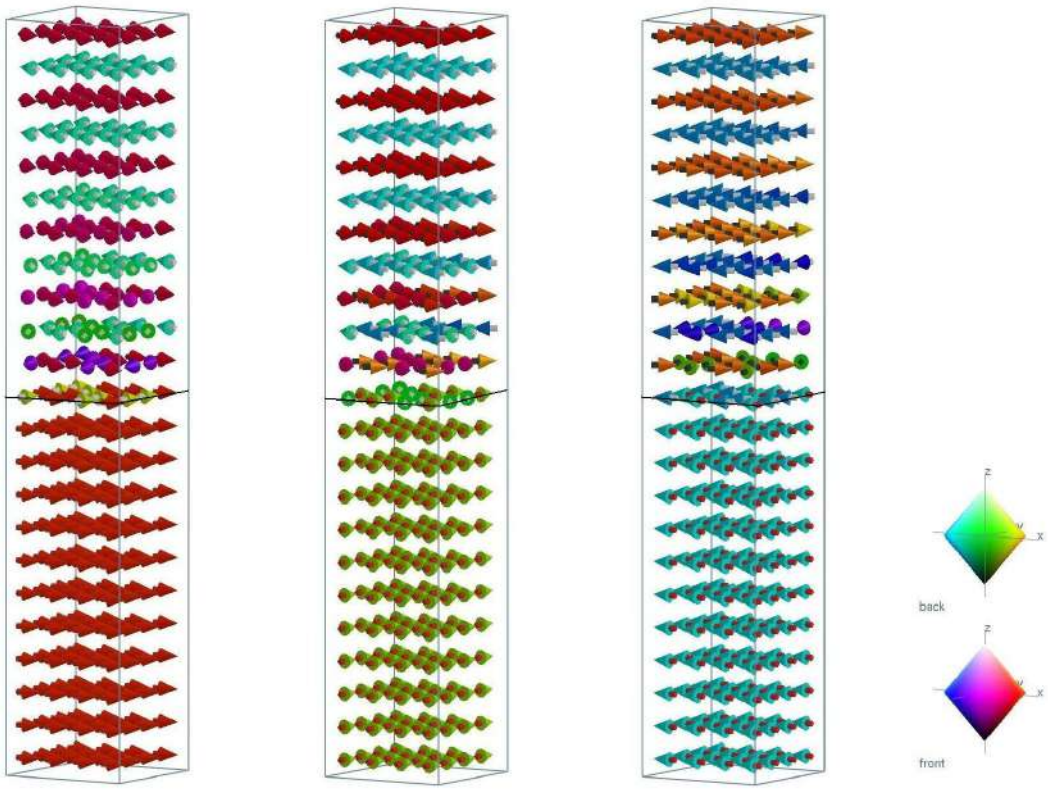

Fig. 3.4: *Spin configuration for a AFM/FM bilayer in three different states: positive saturation (left), zero applied field (middle), negative saturation (right); FM thickness is 6nm, AFM thickness is 4nm and LS=5.6nm; the lower part of the structure represents the FM layer, the upper part the AFM layer, different colors stand for different spin orientation according to the color coordinate system (*color cone*); the AFM/FM interface is emphasized by a black line.*

lower part of the structure represent the FM layer, the upper part the AFM layer, in the figure different colors stand for different spin orientations according to the *color cones*) when the magnetization of the FM layer shifts (right side of the figure 3.4) no irreversible process happens in the AFM (formation of magnetic domains and domain walls), only the spins close to the interface will slightly rotate and this is a reversible process. Thus with no irreversible processes in the AFM no hysteresis is expected (fig 3.3 the curve for $LS = 5.6nm$).

The fact that there is no magnetic domains or domain walls formation in the AFM is strictly an effect due to the reduced LS. Let us calculate the length of a domain wall in the AFM, using the formula $\delta_{AFM} = \pi\sqrt{A_{AFM}/K_{AFM}}$ we will obtain $\delta_{AFM} \approx 8nm$. Because the thickness of the AFM ($6nm$) is smaller than δ_{AFM} parallel to the interface domain walls can not form in the AFM. Nevertheless the LS of our structure ($5.6nm$) is also smaller than the length of an AFM domain wall, and is not enough to accommodate a perpendicular to the interface domain wall in the AFM. So the finite size of our structure

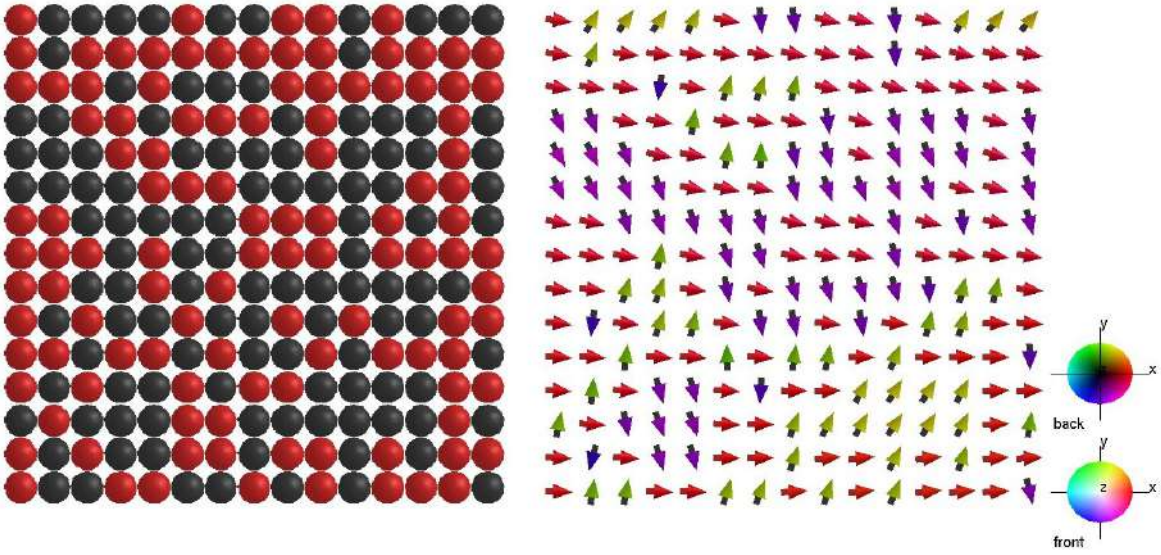

Fig. 3.5: *Interface plane atomic arrangement (left-hand side) for the system with* $t_{AFM} = 4nm$, $t_{FM} = 6nm$ *and* $LS = 20nm$ *, the red dots represent the FM* atoms*, the black ones the AFM* atoms*; corresponding spin configuration in zero applied field, after a previous positive field saturation stage.*

will impose that neither parallel nor perpendicular domain walls to be form in the AFM.

Let us now turn to the structure with $LS = 20\,nm$. Like argued by Malozemoff [9] the interface roughness will induce a magnetic frustration of the interface spins. This can be observed in fig 3.5 where we present the interface plane spin configuration (right-hand side of the picture) of the structure with $t_{AFM} = 4\,nm$, $t_{FM} = 6\,nm$ and $LS = 20\,nm$, in zero applied field and after a previous positive field saturation stage (the color of spin *tail* indicate the nature of the spin: black for an AFM one and red for a FM one, while the color of the spin *hat* indicates the spatial orientation of the spin, in agrement withe the *color wheel*). In the left-hand of the picture is presented the corresponding *atomic* configuration of the interface plane, the red dots represent FM *atoms* as the black ones represent AFM *atoms*. One can observed that the FM spins are likely to remain oriented along the easy anisotropy axis (parallel with Ox), while the AFM spins, due to the magnetic frustration, are oriented align along an axis perpendicular to the easy axis. It can also be seen that a fraction of the AFM spins is oriented along the positive direction of the Oy axis while the other part is oriented along the negative direction of the Oy axis. For continuous film and if the AFM will remain in a single domain state, in average the number of AFM interfacial spins pointing in one direction will be the same as the number pointing in the opposite one, thus the bias filed will be zero since there is no AFM net magnetic moment at the interface. This is true only for a infinite layer.

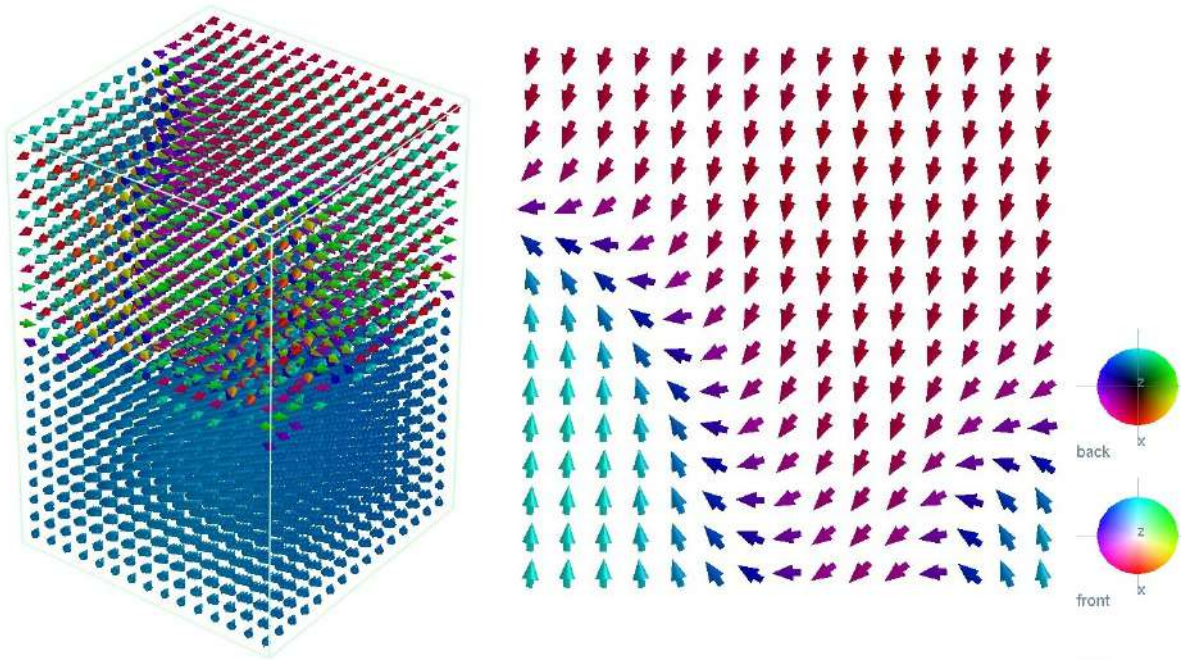

Fig. 3.6: *Spin configuration (left-hand side) for a AFM/FM bilayer (FM thickness is 6nm, AFM thickness is 4nm and LS=20.0nm), in negative field when the FM magnetization starts to rotate; and the top most layer (right-hand side) of the structure in the same conditions.*

In our case finite size effects will intervene in the sense that there will not be a perfect compensation of the interface AFM spins due to the fact that the average is no longer done over an infinite area but over a finite one. Thus there will always remain a fraction of uncompensated AFM spins at the interface that will create a bias filed.

Because δ_{AFM} ($\approx 8\,nm$) is smaller than the LS ($\approx 20\,nm$) one can expect the system to relax the magnetic frustration energy by the breaking up of the AFM into domains. In the figure 3.6 is presented the spin configuration of the structure with $LS = 20\,nm$ (left-hand side), in negative field, when the FM layer magnetization starts to rotate and a view of the top most layer of the AFM (right-hand) in the same situation. It can clearly be seen that perpendicular to the interface domain walls form starting from the corners of the structure, this is because the edge spins are less pined due to the reduced coordination. This spins can more easily rotate during the magnetization reversal of the FM layer and thus they will become centers for the domain formation. Malozemoff argued that the AFM perpendicular domain wall size is determined by a balance between a gain in FM/AFM interfacial energy provided by aligning the local net AFM moment with the FM magnetization and an energy cost due to domain walls formation in the AFM, following his arguments one can calculate the typical size of an AFM domain to be:

$$D_{AFM} = \pi^2 J_{AFM} t_{AFM} / (J_{INT}) \tag{3.1}$$

where J_{AFM} is the exchange constant in the AFM and J_{INT} is the interfacial exchange constant (for details about the derivation of the above relation see appendix B). In our case the size of a domain in the AFM is found to be $D_{AFM} \approx 80\,nm$ (nevertheless we have to take into account that the formula for D_{AFM} was derived for a continuous film, and not for a nanostructure, where the finite size effects have to be taken into account thus this value is not to be taken as exact, but only as an estimation of the order of magnitude of the AFM perpendicular domain size in nanostructures). Hence since the lateral size (LS) is smaller than the typical AFM domain length (D_{AFM}) the formation of the domain walls is energetically unfavorable these existing only in a metastable phase.

This fact is emphasized in figure 3.7 where we present (upper part) the spin configuration, of a three atomic planes cut into the structure (the cut is perpendicular to the interface), in three different conditions: in positive field saturation, when domain walls form and in negative field saturation. A view of the AFM top most layer in the same

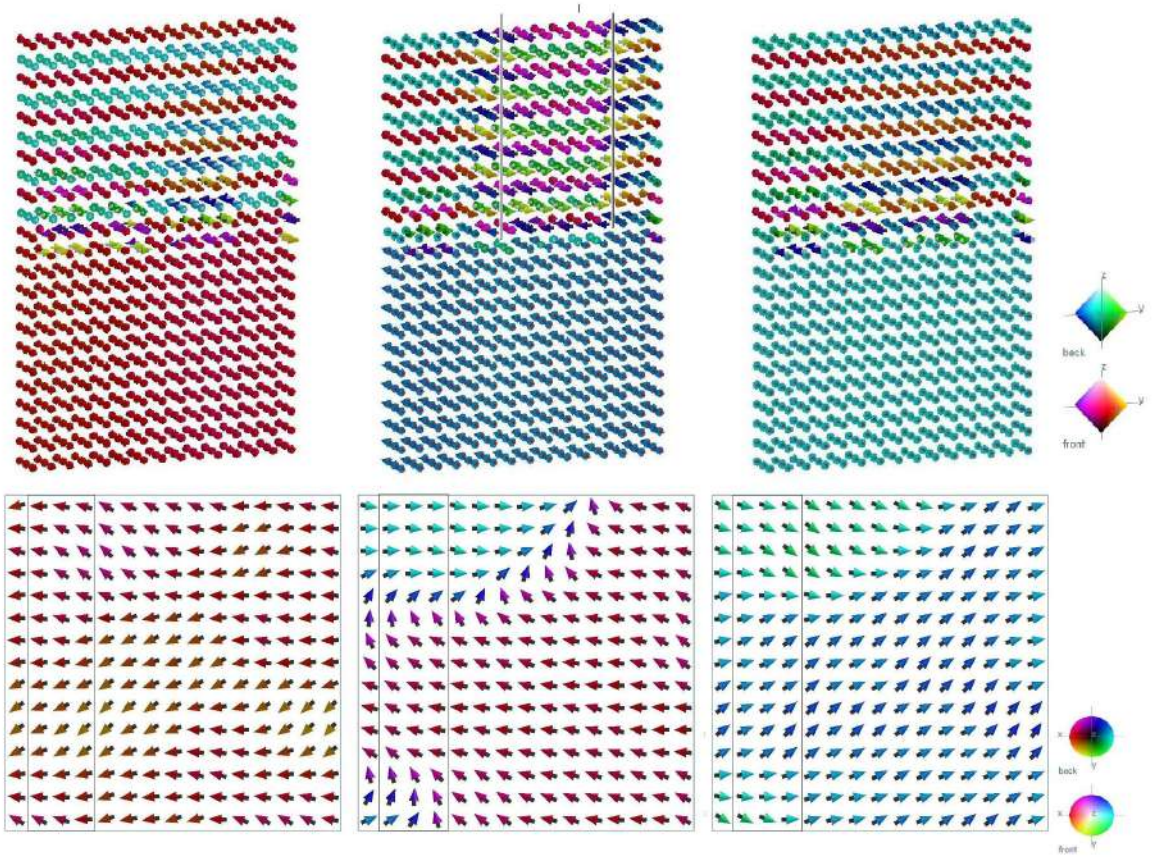

Fig. 3.7: *Spin configuration for an* atomic *situated in the AFM layer in three different situations: positive saturation (left), when domain walls form (middle), negative saturation (right); FM thickness is 6 nm, AFM thickness is 4nm and LS=20.0nm.*

conditions (fig. 3.7 the bottom part) it is also presented. The spot where the *cut* was made is emphasized, on the AFM top most layer by two black lines. One can observe

that in positive saturation (upper-left-hand side of the figure 3.7) the AFM spins close to the interface are are to some extent rotated from the easy anisotropy axis (different spins colors means different orientation), this is due to the fact that AFM spins from the interface are frustrated and this this frustration energy will spread throughout a number of atomic planes close to the interface. While the spins that are *far* from the interface (see the bottom-left-hand side of the fig. 3.7) are likely to remain oriented along the easy anisotropy axis. As the FM layer magnetization starts to rotate a perpendicular domain wall will form in the AFM (fig. 3.7 upper-part middle), in the figure the wall is highlighted by two black lines drawn along the wall. The wall extends trough the whole AFM layer and can be observed on the top most layer of the AFM (fig. 3.7 bottom-middle part) Once the FM layer magnetization completely turns around the domain wall will collapse (fig. 3.7 right-hand side) once with the flipping of the AFM spin lattice. The formation and the collapse of domain walls is nevertheless a irreversible event. Hence the existence of perpendicular domain walls in the AFM, once the LS is large enough to accommodate them, stands for the occurrence of hysteresis (fig. 3.3 the curves for $LS \geq 20\,nm$).

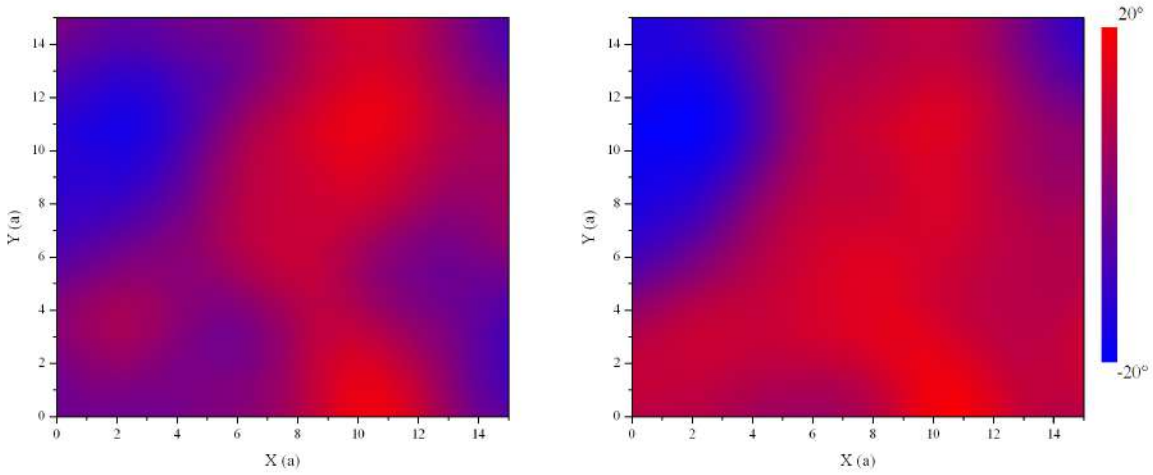

Fig. 3.8: *AFM top most layer spin misalignment plot map, before (left-hand side) and after (right hand side) the FM layer magnetization reversal; FM thickness is 6nm, AFM thickness is 4nm and LS=20.0nm.*

One can argue that if the AFM spin lattice flips the system will jump from one configuration to another symmetrically and energetically equivalent one, and this will lead to no bias. However we can see from the figure 3.8, where we plot the AFM top most layer misalignment from the easy anisotropy axis before (left-hand side) and after (right-hand side) the reversal of the FM magnetization, that although the two configurations are to some extent close a small difference exists that will guarantee that these are not energetically equivalent assuring the presence of exchange bias.

In the figure the 3.9 is presented the spin configuration of the top most layer of the

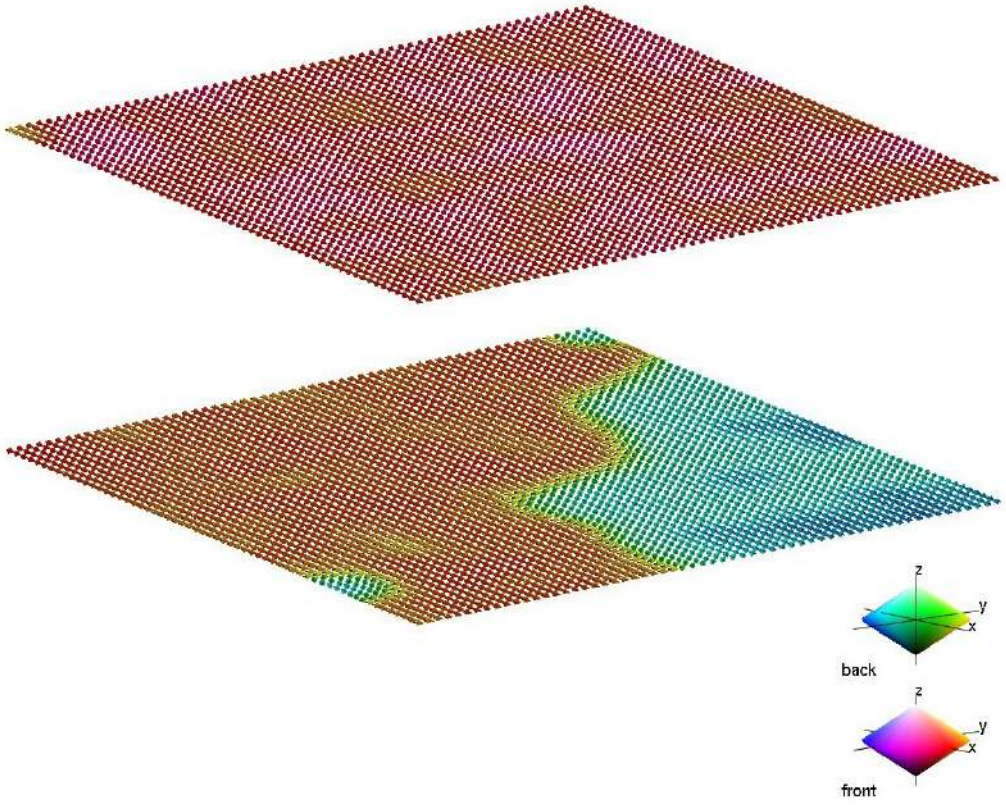

Fig. 3.9: *The spin configuration of the system top most layer of the AFM in positive saturation (upper-part) and after the full reversal of the FM layer magnetization (lower-part); the lateral size of the structure is* $80\,nm$ *and* $t_{AFM} = 4\,nm$.

AFM, in positive field saturation (upper-part) and after the complete reversal of the FM layer magnetization (lower-part), for the structure with $LS = 80\,nm$. One can observe that once with the reversal of the FM layer magnetization domains will form in the AFM. Since the LS of the system is now comparable withe the typical AFM domain size (D_{AFM}), the domain walls will gain stability compared with the structures with a smaller LS and for this reason they will not collapse after the total reversal of the FM layer magnetization

In conclusion for the structure with $t_{AFM} = 4nm$, depending on the LS, three different spin configuration of the AFM layer, during the reversal of the FM layer magnetization, were observed. For the systems with $LS < 20\,nm$, because of the reduced lateral size, no domain walls form in the AFM. For the structures with LS between 20 and $60\,nm$ domain walls form in the AFM that will eventually collapse, once the magnetization of the FM layer is fully reversed. Finally for the dots with $LS > 80\,nm$, due to the fact that LS becomes comparable with D_{AFM}, more stable domain walls form in the AFM, that will exist even after the FM magnetization shifts.

3.1.2 The system with the AFM layer thickness of 10 nm

In order to observed, as well, the effects of the AFM layer thickness on the exchange

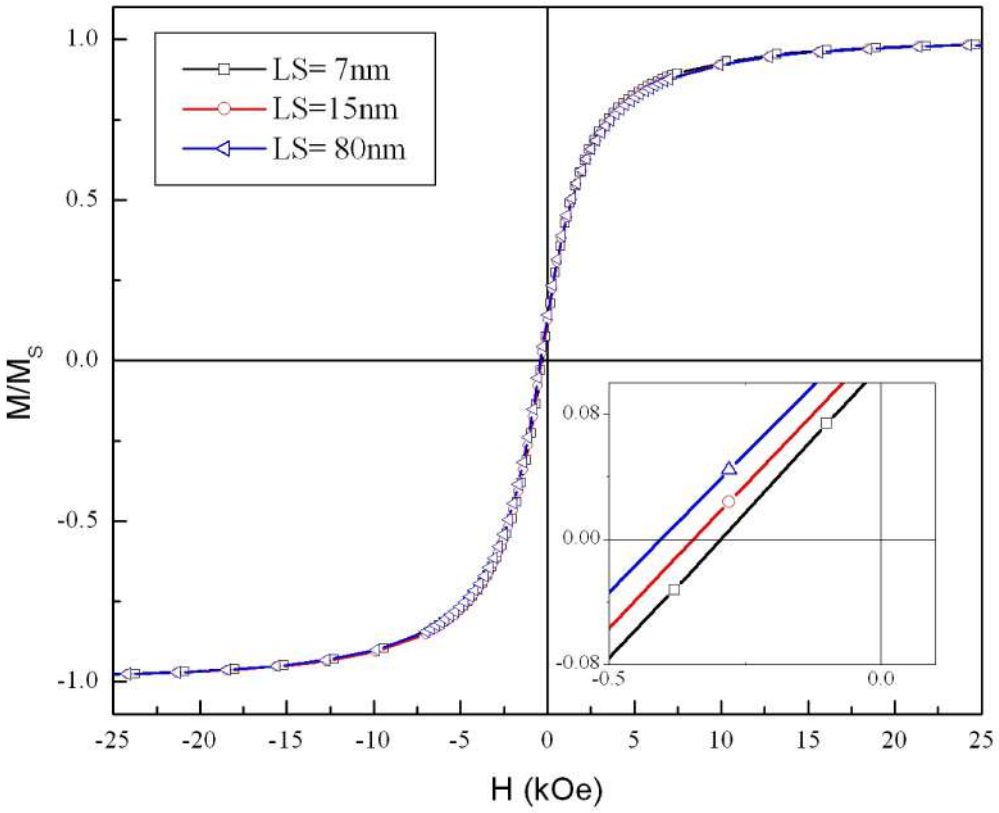

Fig. 3.10: *Hysteresis cycles for an AFM/FM bilayer; FM thickness is 6 nm, AFM thickness is 10nm and LS=7, 15, and 80 nm. The inset shows a zoom of the curves intersection with the* $M = 0$ *axis.*

bias, we have calculated hysteresis cycles for systems with a FM layer thickness of 6 nm, a AFM layer thickness of 10 nm and a lateral size comprised between 7 and 100 nm. Obtained hysteresis cycles are presented in the figure 3.10 (to maintain the clarity of the graph only three curves are presented). A striking feature of the obtained curves is that no one presents hysteresis, not even those for a $LS = 80\,nm$ or $LS = 100\,nm$. From this one can concluded that domain walls do not form in the AFM for such a thickness of the AFM layer. This can be due to the fact that hat with increasing AFM thickness it becomes more and more difficult to form domain walls since these are oriented perpendicular to the interface extending through the whole AFM layer. The corresponding domain-wall energy increases with thickness but can be reduced by reducing the number of domain walls so by the formation of larger domains. However using the relation 3.1 we can calculate the domain size to be $\approx 200\,nm$, a value that is approximatively two times grater than the lateral size of our largest structure ($LS =$

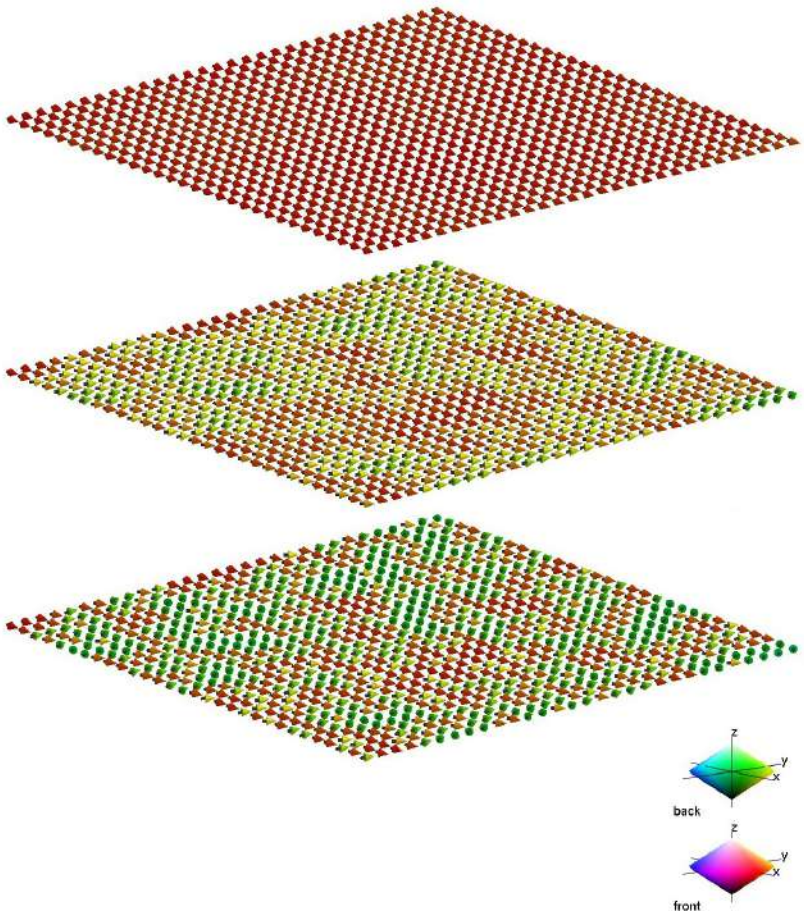

Fig. 3.11: *Spin configuration, after the reversal of the FM layer magnetization, of the top most layer of the AFM (upper part), of a layer in the middle of the AFM (middle part) and of the first AFM plane (lower-part); the lateral of the system is* 80 nm *and* $t_{AFM} = 10\,nm$.

100 nm), so one might expect that the formation of domain walls in the AFM to be a completely energetically unfavorable event.

In the figure 3.11 we present the spin configuration, after the reversal of the FM layer magnetization (the FM magnetization in the negative Ox axis direction), of the top most layer of the AFM (upper part), of a layer in the middle of the AFM (middle part) and of the first AFM plane (lower-part), for a lateral size of 80 nm . The spin configuration is in totaly agreement with our previous remarks. Due to the interfacial frustration (see the spin configuration for the first AFM plane), local variation of the AFM order will spread into de AFM (see the spin configuration of the AFM middle layer) but no magnetic domain wall to extend through the whole AFM layer will form (see the spin configuration of the AFM top most layer).

In conclusion for the structure with $t_{AFM} = 10\,nm$, no matter on the LS, the spin

behavior of the AFM layer, during the reversal of the FM layer magnetization, is approximately the same. This is due to the fact that for such a AFM thickness the domain size it is about two times grater than our largest simulated structure, and this will render the formation of domain walls energetically unfavorable.

3.1.3 The system with the AFM layer thickness of 2 nm

In the figure 3.12 we present two hysteresis cycles obtained for a system with a AFM

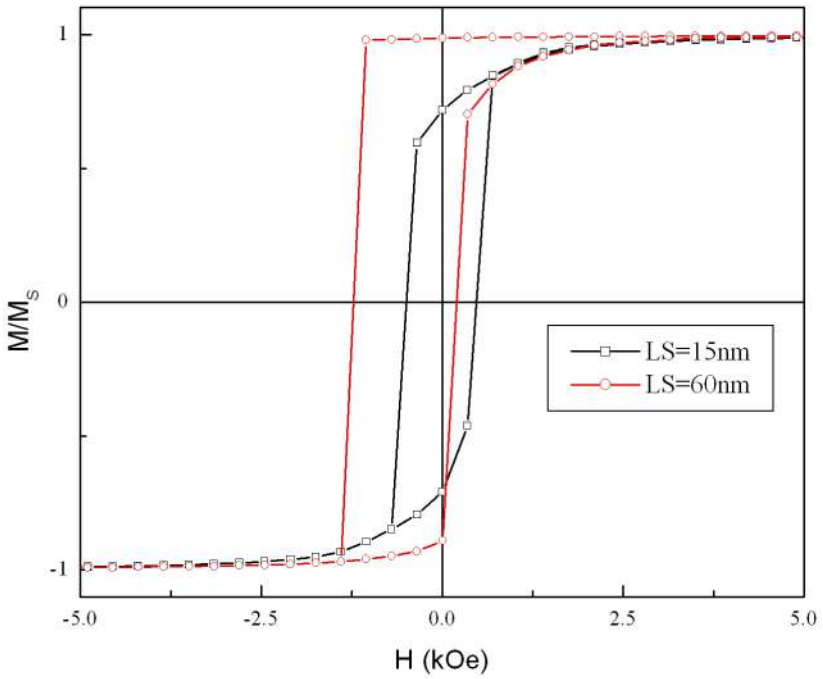

Fig. 3.12: *Hysteresis cycles for an AFM/FM bilayer; FM thickness is 6 nm, AFM thickness is 2nm and LS=15, and 60 nm.*

thickness of 2 nm. For such a t_{AFM}, no matter on the LS all cycles present hysteresis. However for lateral sizes smaller than 40 nm, the curves present no shift. From the observation of the spin configuration we have concluded that for structures with a $LS < 15\,nm$ the AFM, no domain wall forms in the AFM and that the spin lattice has a reversible flip once the FM magnetization reverses. For LS between 15 and 60 nm domain walls form in the AFM (see fig. 3.13) but they are simply not enough pinned to remain in place, they will move in a reversible way, to a new position, thus giving rise to coercivity without bias. Above this LS, some of the domain state magnetization rapidly becomes irreversible leading to bias.

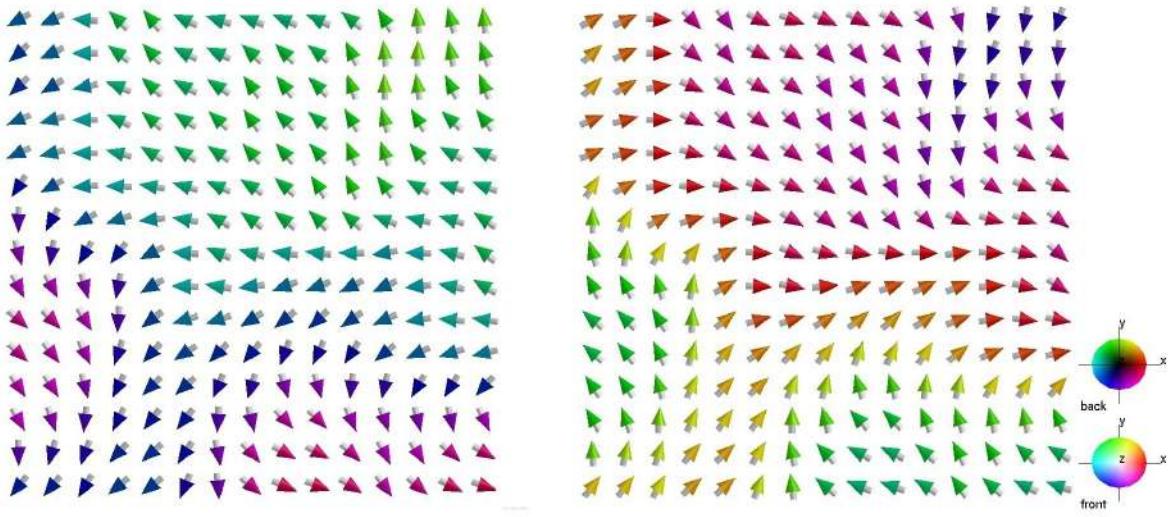

Fig. 3.13: *The AFM top-most layer spin configuration before (left) and after (right) the FM layer magnetization reversal; lateral size is* $LS = 20\,nm$ *an* $t_{AFM} = 2\,nm$.

3.2 The variation of the exchange bias field with the lateral size and the thickness of the AFM layer

The exchange bias filed variation on the lateral size of the system, for different AFM layer thicknesses is plotted in figure 3.14.

For small AFM layer thicknesses ($2-3\,nm$), and for lateral sizes of the system smaller than $15\,nm$ H_E is practically equal to zero. As we have seen in the previous section, for such dimensions, once with the reversal of the FM layer magnetization, no domain walls form in the AFM and even more the spin lattice of the AFM flips, from one spin configuration to another energetically equivalent one. When the system area is increased (LS between 20 and $60\,nm$ for $t_{AFM} = 2\,nm$ and LS between 20 and $40\,nm$ for $t_{AFM} = 3\,nm$) domain walls start to form in the AFM. However this domains walls have a poor stability (see sec. 3.1.3), but once the LS is increased they will be more and more pinned and thus this will lead to an increase in H_E. After the installation of the domain walls formation state, and after the domains have achieved stability H_E will be roughly independent of LS.

The curves behavior for AFM layer thicknesses between 4 and $6\,nm$ can be described as follows: the first ascendent part of the curves ($LS < 20\,nm$) corresponds to the transition between the no AFM domain formation state and and no AFM spin lattice flip (see for example fig. 3.4) to the the AFM domain walls formation state (see for example fig. 3.7); the second ascendent part (LS between 40 and $60\,nm$) corresponds to the situation where the AFM domain walls gain in stability; for LS between 60 and $100\,nm$ the AFM domain walls formation state is fully achieved and the domains have reached a relative stability, so in this situation H_E remains roughly constant.

In the figure 3.15 we present a map plot of the spin misalignment, from the easy

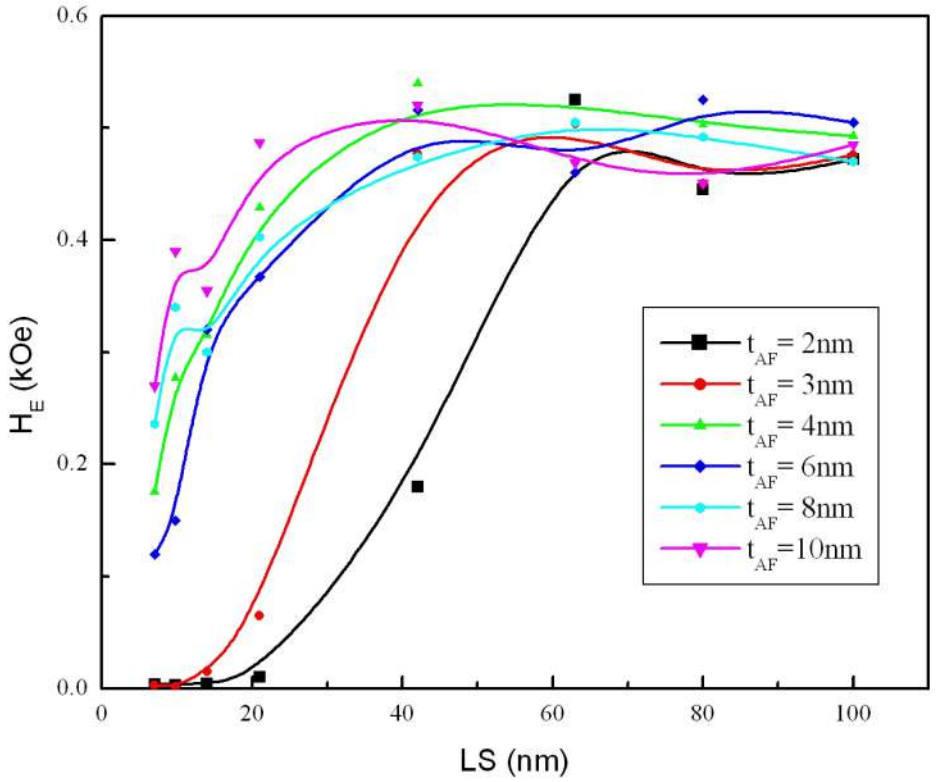

Fig. 3.14: *Dependence of the exchange bias field,H_E, on the lateral size (LS) for the system with $t_{AFM} = 4\,nm$, $t_{FM} = 6\,nm$. The lines have no physical meaning.*

anisotropy axis, of the AFM top most layer of the structure with $t_{AFM} = 8nm$, for 4 different sizes: $LS = 7\,nm$, $20\,nm$, $40\,nm$, and $60\,nm$, after the reversal of the FM layer magnetization. We can see from the figure that for the smallest lateral size ($LS = 7nm$) there is an important degree of misalignment (in average $\approx 6°/spin$) this can be connected to the fact that for such a LS the number of surface spins (*less pinned spins*) comparative to the number of spins bulk spins is relatively high (there are $\approx 35\%$ bulk spins). As the size increases ($LS = 20nm$ and $LS = 40nm$) the misalignment reduces (in average $\approx 3°/spin$ for $LS = 40nm$), again if we calculate the number of bulk spins relative to the total number we will obtain a value more than two times grater than in the case of $LS = 7\,nm$ (approximately 83%), and this enhanced number of *pinned spins* can be accounted for the relative increase in the alinement of the AFM spins. So the spins from the *interior* of the layer will gain in pinning and thus giving rise to an increase in H_E (see fig. 3.14). We can also observe that the misalignment is concentrated on the sides of the structure because there the spins ar less coordinated and hence more easily rotatable. Increasing even more the size of the structure ($LS = 60nm$) domain

walls form in the AFM, starting from the corners, where the spins are less pinned.

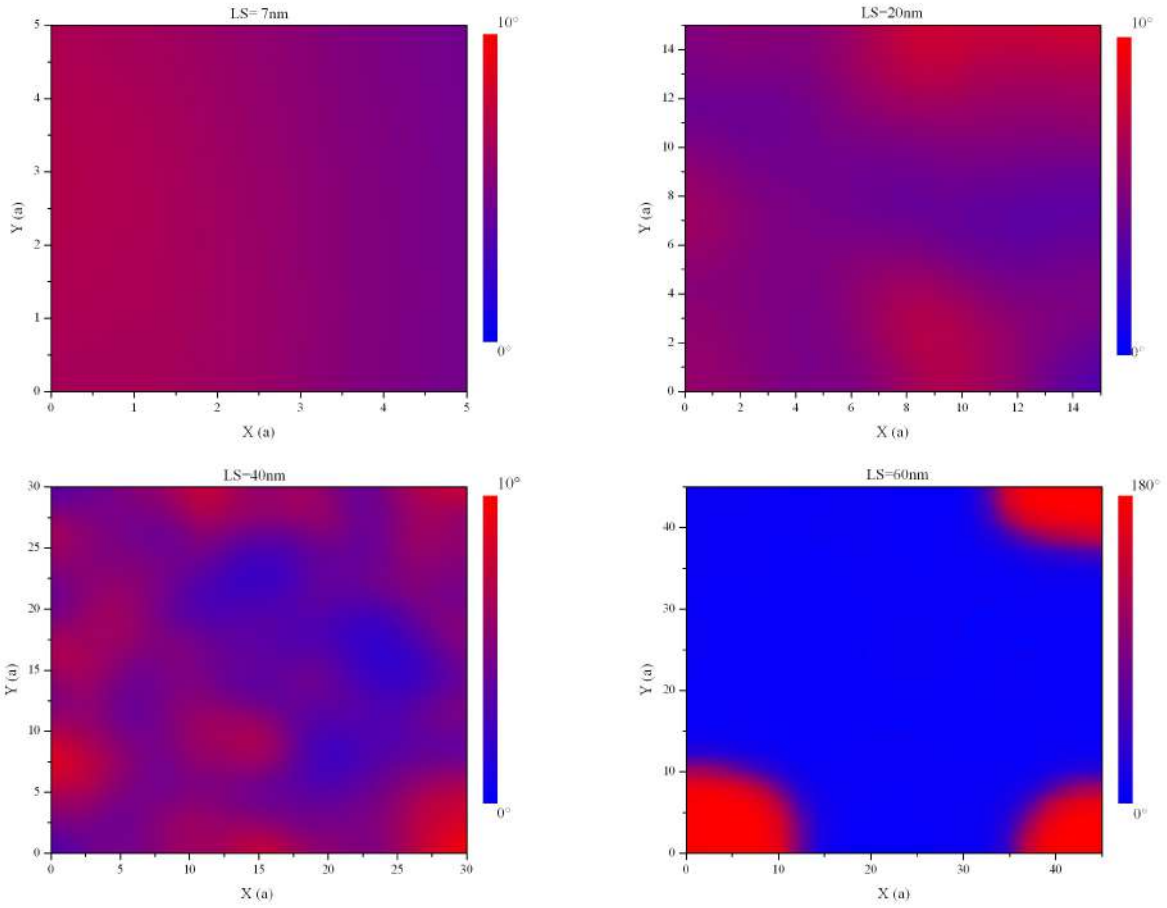

Fig. 3.15: *Map plot of the AFM top most layer spin misalignment configuration for four different lateral sizes of the structure:* $LS = 7\,nm$, $20\,nm$, $40\,nm$, *and* $60\,nm$. *The thickness of the AFM layer is* $8\,nm$.

Because of the fact that no matter on the LS, for $t_{AFM} = 10\,nm$, when the FM magnetization reverses the AFM spin behavior is practically the same (no AFM spin flip and no domain formation, see sec. 3.1.2 and figure 3.11), one may expect that the curve for $t_{AFM} = 10\,nm$ to be to some extent constant. However this is not the case, as we can see from the figure 3.14, for low lateral dimensions H_E is smaller than for larger lateral sizes. One can consider that this is an effect of the *surface* spins, due to the fact that their coordination is smaller than that of the *bulk* spins they are less pinned. In fact if one calculates the rapport between the *bulk* and the total number of spins for $LS = 7\,nm$ and $LS = 20\,nm$ one will obtain: 0.34 and respectively 0.72 . If we divide this numbers we will obtain: 0.47. Let as calculate the rapport between the H_E for a $LS = 7\,nm$ and a $LS = 20\,nm$: $0.27/0.496 = 0.54$. We can see that this numbers are roughly close so to some degree one can ascribe the comportment of the H_E for small

LS values to the relatively increased numbers of AFM *surface* spins. Nevertheless this reduced *bulk* spins effect is present also in systems with lower t_{AFM}, but there we will have in addition a decrease in H_E due to the different AFM spin configuration behavior, on the reversal of the FM magnetization, for various AFM layer thicknesses.

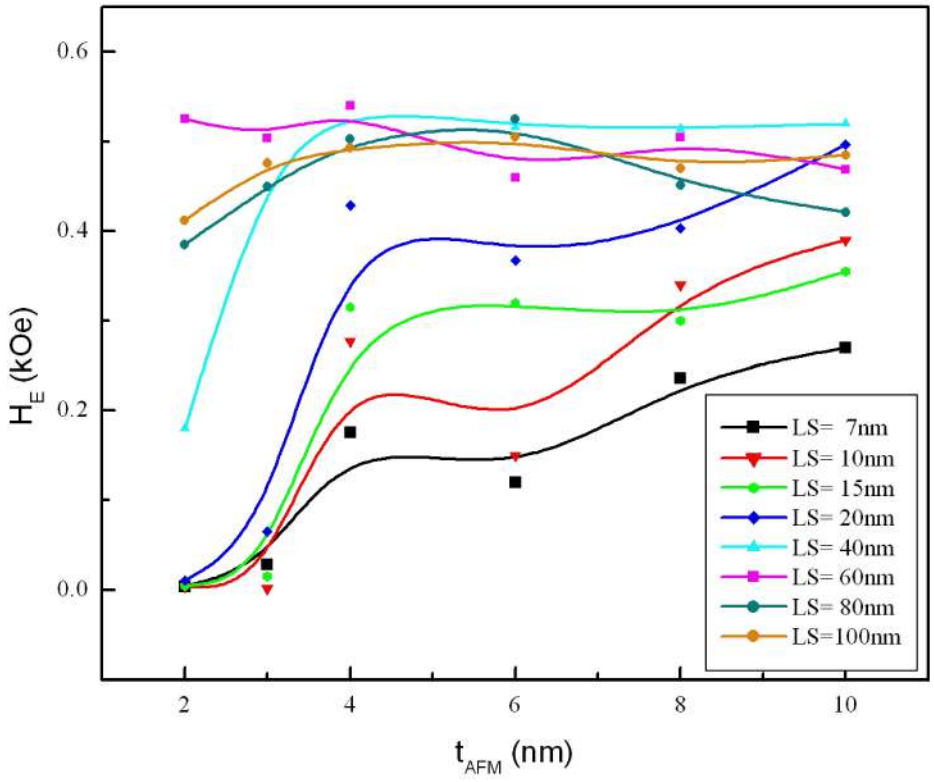

Fig. 3.16: *Dependence of the exchange bias field,H_E, on the thickness of the AFM layer for a lateral size of the system of $LS = 80\,nm$, $40\,nm$, $20\,nm$, $15\,nm$ and $7\,nm$. The lines are guide to the eye.*

In the figure 3.16 we present the exchange bias field dependence on the t_{AFM} for various system lateral sizes.

As expected for large lateral sizes ($LS > 40\,nm$), when the system can accommodate AFM perpendicular domain walls H_E is roughly constant. Nonetheless for large AFM thicknesses a small decrease in H_E is observed. Above this thickness the decline in H_E is caused by the fact that with increasing AFM thickness it becomes more and more difficult to form domain walls, since these are oriented perpendicular to the interface, extending through the whole AFM layer. So by reducing the number of domain walls (to none for the most thick layer) the interface AFM magnetization will be reduced and, hence, the bias field.

For small lateral sizes ($LS < 20\,nm$) H_E is increasing with increasing thickness, this can be due to the fact that the pinning of the AFM spin increases with increasing AFM thickness (the number of *surface* spins relative to the *bulk* ones is decreasing).

The H_E variation on the thickness of the AFM layer was investigated experimentally for a lateral size of $90\,nm$ [7]. The authors reported a H_E roughly independent of the AFM thickness (for thicknesses between 6 and $20nm$), this behavior is in total agreement with our simulations (see fig. 3.16). They have accounted this for the fact that due to the fact that the bilayer lateral size is smaller than the AFM domain size the AFM remains single-domain, thus keeping H_E constant. Our simulation have confirmed this assumption. AS we have seen for the systems with LS between 80 and $100\,nm$ and for AFM thicknesses larger than $6\,nm$ domains do not form in the AFM (however domain walls have formed in the AFM for the structures with t_{AFM} between 6 and $8nm$, but for each case approximatively 90% from the AFM surface remained single-domain).

Conclusions

The objective of this internship was the investigation of the finite size effects on the exchange bias in an AFM/FM bilayer using atomistic numerical simulations.

The size effects study on exchange bias was done on systems the FM layer thickness constant (6 nm equivalent with 11 atomic planes) while the thickness of the AFM layer was varied between 2 an 10 nm (6 to 29 atomic planes), also the lateral dimension of the structure was swept between 7 and 100 nm (corresponding to 5 respectively 75 *atomic* planes.

We have observed that the H_E has different compartments with the LS for different t_{AFM}. For small AFM layer thicknesses ($2-3\,nm$), and for lateral sizes of the system smaller than $15\,nm$ once with the reversal of the FM layer magnetization, the spin lattice of the AFM flips from one spin configuration to another energetically equivalent one leading to no bias. When the system area is increased (LS between 20 and $60\,nm$ for $t_{AFM}=2\,nm$ and LS between 20 and $40\,nm$ for $t_{AFM}=3\,nm$) domain walls start form in the AFM, their stability is increased once with the LS and this will lead to an increase in H_E. After the installation of the domain walls formation state, and after the domains have achieved stability H_E will be roughly independent of LS.

For thicker AFM layers (between 4 and $8\,nm$) the curves have a first ascendent part of the corresponding to the transition between the no AFM domain formation state and and no AFM spin lattice flip to the the AFM domain walls formation state; the second ascendent part corresponds to the situation where the AFM domain walls gain in stability; the final part of the curves stands for the situation when AFM domain walls formation state is fully achieved and the domains have reached a relative stability, so in this situation H_E remains roughly constant.

For even thick layers ($LS=100\,nm$) no domain walls form in the AFM, but the curve has a decrease for low LS values we attributed this behavior to the relatively increased number of *surface* spins for small LS.

As for the comportment of the H_E with the t_{AFM} we have obtained two behaviors depending on the lateral sizes of the system. For large lateral sizes ($LS>40\,nm$), when the system can accommodate AFM perpendicular domain walls H_E is roughly constant. For small lateral sizes ($LS<20\,nm$) H_E is increasing with increasing thickness, this was attributed to the increased coercivity due to the relative increased number of *bulk* spins.

Appendix A: Renormalization of the material parameters

In order to facilitate the numerical calculation the *real* dimensions of the systems were reduced by operating a *renormalization* of the system.

Let us consider two *spins*, each standing for $m \times m \times n$ *atomic spins* (see figure A-1).

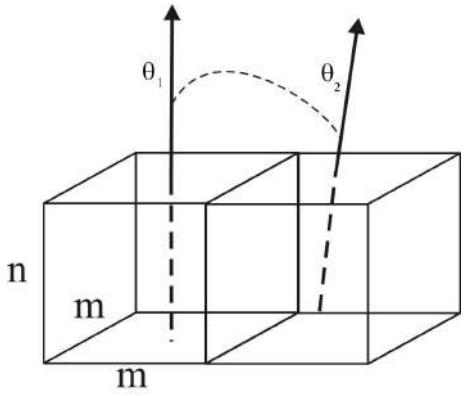

Fig. A-1: *Two* renormalized spins *each standing for* $4 \times 4 \times 1$ atomic spins

For the *atomic* anisotropy we can write:

$$K = \sum_i K_{at} = m^2 \times n \times K_{at} \tag{A-2}$$

For the magnetic moment we can write, approximating that all $m \times m \times n$ spins that form *renormalized spin* are parallel:

$$\mu = \sum_i \mu_i = m^2 \times n \times \mu^{at} \tag{A-3}$$

Considering that the angle between the *atomic spins* that constitute a *renormalized spin* is the same, taking into account the fact that between two *renormalized spin* there are m *atomic spins*, one can write (for the in-plane direction) for the exchange energy:

$$E_{ech} = J_{at} \sum_{i,j} cos\left(\theta_i - \theta_i\right) \approx J_{at} \sum_{i,j} \left[1 + \frac{\left(\theta_i - \theta_i\right)^2}{2}\right] = n \times J_{at} \times \frac{\left(\theta_1 - \theta_2\right)^2}{2} \tag{A-4}$$

However, for the in-plane direction, we can write:

$$E_{ech} = J_{\parallel}^{*} \times \frac{(\theta_1 - \theta_2)^2}{2} \tag{A-5}$$

so the new in-plane exchange constant will be:

$$J_{\parallel}^{*} = n \times J_{at} \tag{A-6}$$

In the same way it can be shown that the out-of-plane exchange constant can be written as:

$$J_{\perp}^{*} = \frac{m^2}{n} \times J_{at} \tag{A-7}$$

Appendix B: The calculation of the size of an AFM domain wall

According to Malozemoff [9],[10] due to the random coupling through the interface the

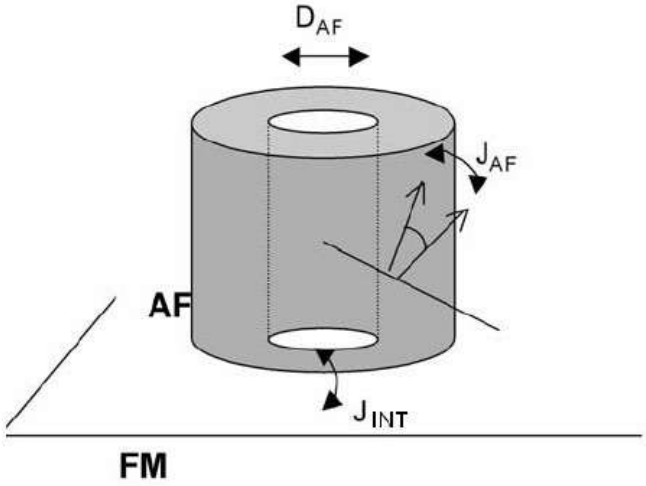

Fig. B-1: *Schematic representation of an AFM cylindrical domain.*

AFM spin lattice breaks up into domains, the size of which is determined by a balance between a gain in AFM/FM interfacial energy provided by aligning the local net AFM moment with the FM magnetization and an energy cost due to domain walls formation in the AFM. It can be argued that for a given AFM domain size, D_{AFM}, the number of AFM moments at the AFM/FM interface is

$$N = (D_{AFM}/a)^2$$

, where a is the distance between AFM spins. The interface random field energy can be expressed as $-J_{INT}/N^{1/2}$, where J_{INT} is the exchange constant of the FM/AFM coupling. Therefore, the interface coupling energy per unit area is:

$$\sigma_{AFM/FM} = -J_{INT}/aD_{AFM} \tag{B-2}$$

Hence, the interface coupling energy decreases when increasing the AFM domain size. Additionally, the domain wall energy in the AFM, assuming that domain walls

are oriented perpendicular to the AFM/FM interface and extending through the whole AFM layer can be written the following way:

$$\sigma_{DW} = \sigma^0_{DW} = \frac{S_{DW}}{S}$$

where,

$$\sigma^0_{DW} = J_{AFM}\frac{\sqrt{N}}{2}\frac{1}{a^2}\frac{\delta\phi}{2}$$

and if we consider the angle between neighboring spins constant through all the wall:

$$\delta\phi = \pi\frac{a}{D_{AFM}}$$

and

$$S = \pi\left(\frac{D_{AFM}}{2}\right)^2 \qquad S_{DW} = \pi D_{AFM} t_{AFM}$$

so:

$$\sigma_{DW} = \pi^2 J_{AFM}/(4aDAFM) \tag{B-3}$$

This equation shows that AFM domain walls are more difficult to create for thicker AFM layers. In fact,σ_{DW} can be minimized by enlarging the AFM domain size. By minimizing the total energy per unit AFM/FM interface area, one obtains the following relationship between the AFM domain size and t_{AFM}:

$$D_{AFM} = (J_{AFM}/INT)\pi^2 t_{AFM} \tag{B-4}$$

Bibliography

[1] S.S.P. Parkin B. Dieny, V.S. Speriosu. *Phys. Rev. B.*, **43**: 1297, (1991).

[2] A.E. Berkowitz and K. Takano. *J. Magn. Magn. Mater.*, **200**: 552, (1999).

[3] H. C. Siegmann D. Mauri. *J. Appl. Phys*, **192**: 203, (1999).

[4] E. du Tremolet de Lacheisserie. *Magnetism-Fondamentals*. Springer, 2005.

[5] F. Ernult. *Anisotropie d'exchange et frustration magnetique dans de bicouches ferro/antiferro et des tricouches ferro/antiferro/ferro*. these de l'Universite Joseph Fourier de Grenoble, 2002.

[6] J. Nogués et al. Exchange bias in nanostructures. *Physics Reports*, **422**: 65, (2005).

[7] V. Baltz et al. *Phys. Rev. Lett.*, **94**: 117201, (2005).

[8] B.J. Hikey M. Ali, C.H. Marrows. *Phys. Rev. B.*, **67**: 172405, (2003).

[9] A.P. Malozemoff. *Phys. Rev. B.*, **35**: 3679, (1987).

[10] A.P. Malozemoff. *J. Appl. Phys*, **63**: 3874, (1988).

[11] A.P. Malozemoff. *Phys. Rev. B.*, **37**: 7673, (1988).

[12] W. H. Meiklejohn and C. P. Bean. *Phys. Rev.*, **105**: 904, (1956).

[13] J. Nogués and I. K. Schuller. *J. Magn. Magn. Mater.*, **192**: 203, (1999).

[14] R. Coehoorn R. Jungblut. *J. Appl. Phys.*, **62**: 3047, (1987).